
BNAS v2: LEARNING ARCHITECTURES FOR BINARY NETWORKS WITH EMPIRICAL IMPROVEMENTS

Dahyun Kim
GIST, South Korea
killawhale@gm.gist.ac.kr

Kunal Pratap Singh
Allen Institute for AI
kunals@allenai.org

Jonghyun Choi
GIST, South Korea
jhc@gist.ac.kr

ABSTRACT

Backbone architectures of most binary networks are well-known floating point (FP) architectures such as the ResNet family. Questioning that the architectures designed for FP networks might not be the best for binary networks, we propose to search architectures for binary networks (BNAS) by defining a new search space for binary architectures and a novel search objective. Specifically, based on the cell based search method, we define the new search space of binary layer types, design a new cell template, and rediscover the utility of and propose to use the *Zeroise* layer instead of using it as a placeholder. The novel search objective *diversifies early search* to learn better performing binary architectures. We show that our method searches architectures with stable training curves despite the quantization error inherent in binary networks. Quantitative analyses demonstrate that our searched architectures outperform the architectures used in state-of-the-art binary networks and outperform or perform *on par* with state-of-the-art binary networks that employ various techniques other than architectural changes. In addition, we further propose improvements to the training scheme of our searched architectures. With the new training scheme for our searched architectures, we achieve the state-of-the-art performance by binary networks by outperforming all previous methods by non-trivial margins.

1 Introduction

Increasing demand for deploying high performance visual recognition systems encourages research on efficient neural networks. Approaches include pruning [1], efficient architecture design [2–4], low-rank decomposition [5], network quantization [6–8] and knowledge distillation [9, 10]. Particularly, network quantization, especially binary or 1-bit CNNs, are known to provide extreme computational and memory savings. The computationally expensive floating point convolutions are replaced with computationally efficient XNOR and bit-count operations, which significantly speeds up inference [7]. Hence, binary networks are incomparable with efficient floating point networks due to the extreme computational and memory savings.

Current binary networks, however, use architectures designed for floating point weights and activations [7, 11–13]. We hypothesize that the backbone architectures used in binary networks may not be optimal for binary parameters as they were designed for floating point ones. Instead, we may learn better binary network architectures by exploring the space of binary networks.

To discover better performing binary networks, we first apply one of the widely used binarization schemes [7] to the searched architectures from floating point NAS which use cell based search and gradient based search algorithms [14–16]. We then train the resulting binary networks on CIFAR10. Disappointingly, the binarized searched architectures do not perform well (Sec. 3). We hypothesize two reasons for the failure of binarized searched floating point architectures. First, the search space used in the floating point NAS is not necessarily the best one for binary networks. For example, separable convolutions will have large quantization error when binarized, since nested convolutions increase quantization error (Sec. 4.1.2). Additionally, we discover that the *Zeroise* layer, which was only used as a placeholder in floating point NAS, improves the accuracy of binary networks when kept in the final architecture (Sec. 4.1.3). Second, the cell template used for floating point cell based NAS methods is not well suited for the binary domain because of unstable gradients due to quantization error (Sec. 4.2).

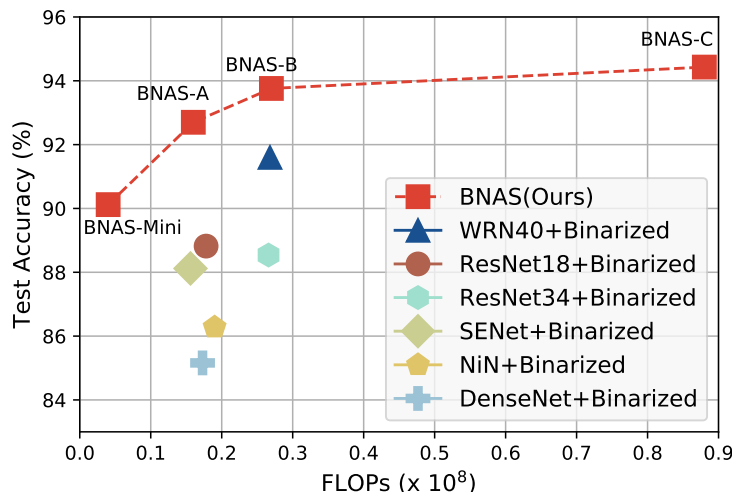


Figure 1: Test accuracy (%) vs. FLOPs on CIFAR10 using the XNOR-Net binarization scheme [7]. Our searched architectures outperform the binarized floating point architectures. Note that our BNAS-Mini, which has much less FLOPs, outperforms all other binary networks except the one based on WideResNet40 (WRN40)

Based on the above hypotheses and empirical observations, we formulate a cell based search space explicitly defined for binary networks and further propose a novel search objective with the diversity regularizer. The proposed regularizer encourages exploration of diverse layer types in the early stages of search, which is particularly useful for discovering better binary architectures. We call this method as Binary Network Architecture Search or *BNAS*. We show that the new search space and the diversity regularizer in *BNAS* helps in searching better performing binary architectures (Sec. 6).

Given the same binarization scheme, we compare our searched architectures to several handcrafted architectures including the ones shown in the Fig. 1. Our searched architectures clearly outperforms the architectures used in the state-of-the-art binary networks, indicating the prowess of our search method in discovering better architectures for binary networks.

In recent research on training binary networks, regularization plays an important role in achieving competitive accuracy [17, 18]. In contrast, we discover a seldomly discussed underfitting problem when training our searched architectures. To mitigate the underfitting problem and ultimately improve the final performance of our searched architectures, we propose *not* to use commonly used regularization techniques during training the searched binary network.

We summarize our contributions as follows:

- We propose the first architecture search method for binary networks. The searched architectures are adjustable to various computational budgets (in FLOPs) and outperform backbone architectures used in state-of-the-art binary networks on both CIFAR10 and ImageNet dataset.
- We define a new search space for binary networks that is more robust to quantization error; a new cell template and a new set of layers.
- We propose a new search objective aimed to diversify early stages of search and demonstrate its contribution in discovering better performing binary networks.
- We observe the underfitting problem in training searched binary networks and propose not to use regularization methods. Our training scheme leads to noticeable improvements in the accuracy of the trained network.

2 Related Work

2.1 Binary Neural Networks

There have been numerous proposals to improve the accuracy of binary (1-bit) precision CNNs whose weights and activations are all binary valued. We categorize them into binarization schemes, architectural modifications and training methods.

2.1.1 Binarization Schemes

As a pioneering work, [6] proposed to use the sign function to binarize the weights and achieved compelling accuracy on CIFAR10. Several attempts have also been made to employ multi-bit weights to enhance the representational capacity of weight-quantized networks [8, 19]. Various approaches quantize both weights and activations, offering higher memory savings and inference speed-up than their weight quantization only counterparts. [20] binarized the weights and the activations by the sign function and use the straight through estimator (STE) to estimate the gradient. [7] proposed XNOR-Net which uses the sign function with a scaling factor to binarize the weights and the activations. They showed impressive performance on a large scale dataset (ImageNet ILSVRC 2012) and that the computationally expensive floating point convolution operations can be replaced by highly efficient XNOR and bit counting operations. Many following works including recent ones [11, 12] use the binarization scheme of XNOR-Net as do we. [21] tried combinations of 1-bit weights and multi-bit low precision activations and gradients to obtain a better trade-off between accuracy and quantization error. [22] approximated both weights and activations as a weighted sum of multiple binary filters to improve performance. [23] employed ternary activations with binary weights for better representation capacity. [24] use reinforcement learning to mine channel-wise interactions to provide prior knowledge which alleviates the inconsistency in signs and preserves information, leading to reduction of quantization error. Very recently, new binarization schemes have been proposed [25, 26]. [25] uses projection convolutional layers while [26] improves upon the analytically calculated scaling factor in XNOR-Net.

These different binarization schemes do not modify the backbone architecture while we focus on finding better backbone architectures given a binarization scheme. A newer binarization scheme can be incorporated into our search framework but that was not the focus of this work.

2.1.2 Architectural Advances in Binary Networks

It has been shown that appropriate modifications to the backbone architecture can result in great improvements in accuracy [7, 11, 12]. [7] proposed XNOR-Net which shows that changing the order of batch normalization (BN) and the sign function is crucial for the performance of binary networks. [27] proposed a local binary convolutional layer to approximate the response of a floating point CNN layer using a non-learnable binary sparse filter and a set of learnable linear filters. [11] connected the input floating point activations of consecutive blocks through identity connections before the sign function. They aimed to improve the representational capacity for binary networks by adding the floating point activation of the current block to the consequent block. They also introduced a better approximation of the gradient of the sign function for back-propagation. [28] ensembled multiple smaller binary networks to achieve comparable performance to floating point networks. [12] used circulant binary convolutions to enhance the representational capabilities of binary networks. [29] proposed a modified version of separable convolutions to binarize the MobileNetV1 architecture. However, we observe that the modified separable convolution modules do not generalize to architectures other than MobileNet. [30] decompose the floating point networks into groups and approximate each group using a set of binary bases. They also introduced a method to learn this decomposition dynamically. These methods do not alter the connectivity or the topology of the network while we search for entirely new network architectures.

2.1.3 Recent Work on Architecture Search for Binary Networks

Recently, [13] performed a hyper-parameter search (*e.g.*, number of channels) using an evolutionary algorithm to efficiently increase the FLOPs of a binarized ResNet backbone. However, they trade more computation cost for better performance, reducing their inference speed up ($\sim 2.7\times$) to be far smaller than other binary networks ($\sim 10\times$). [31] is the first binary networks search method for more than exploring training schemes and regularization terms, and is the earlier conference version of this work. As a concurrent work in the same conference as our previous version, [32] propose to search for binary networks but using a different search space and search strategy than ours. However, the reported accuracy was difficult to reproduce with the given configuration details. We expect further progress in this field with reproducible public codes. Nonetheless, to the best efforts to reproduce the results with many correspondences with the authors, we try to compare ours to their method.

2.1.4 Training Binary Networks

There have been a number of methods proposed for training binary networks in recent literature. [33] showed that quantized networks, when trained progressively from higher to lower bit-width, do not get trapped in a local minimum. [34] proposed a training method for binary networks using Bayesian kernel loss and Bayesian feature loss which act as regularizers under the Bayesian assumption. [17] proposed to regularize the distribution of the intermediate activations of a binary network using the assumption that there exist $+1$ and -1 in equal probability in a binary network. Similarly [35] propose RSign and RReLU as replacements to the traditional Sign and ReLU function respectively to

enable explicit learning of the activation distribution to be as close to floating point networks as possible. [18] also uses the same assumption but they indirectly regularize the activation distribution by their Libra binarization method. They also introduce a better gradient estimator than the standard clip or HardTanh activation function. [36] explore the influence of angular bias on the quantization error and propose a rotated BNN that takes into consideration and improves the performance of the underlying binary network. [37] proposed to pretrain the network with ternary activation which are later decoupled to binary activations for fine-tuning. Recently, [38] proposed to train a binary network using multiple stages and 3 additional networks that need to be trained sequentially before training the binary network. While they show promising gains, it is unclear on how this training scheme can extend to various different architectures and tasks.

Any training methods can be used in our searched networks as we also noted in the earlier version of this work [31]. Interestingly, we discover that our searched architectures achieve satisfactory performance with a much simpler training scheme than the proposed regularizers or training schemes. It may imply that binary network with better architecture may need better fitting rather than using such inductive biases.

2.2 Efficient Neural Architecture Search

We search architectures for binary networks by adopting ideas from neural architecture search (NAS) methods for floating point networks [14, 15, 39–41]. To reduce the severe computation cost of NAS methods, there are numerous proposals focused on accelerating the NAS algorithms [14–16, 41–54]. We categorize these attempts into cell based search and gradient based search algorithms.

2.2.1 Cell Based Search

Pioneered by [39], many NAS methods [14–16, 42, 44–54] have used the cell based search, where the objective of the NAS algorithm is to search for a cell, which will then be stacked to form the final network. The cell based search reduces the search space drastically from the entire network to a cell, significantly reducing the computational cost. Additionally, the searched cell can be stacked any number of times given the computational budget. Although the scalability of the searched cells to higher computational cost is a non-trivial problem [55], it is not crucial to our work because binary networks focus more on smaller computational budgets.

2.2.2 Gradient Based Search Algorithms

In order to accelerate the search, methods including [14–16, 42, 47] relax the discrete sampling of child architectures to be differentiable so that the gradient descent algorithm can be used. The relaxation involves taking a weighted sum of several layer types during the search to approximate a single layer type in the final architecture. [14] uses softmax of learnable parameters as the weights, while other methods [15, 16, 47] use the Gumbel-softmax [56] instead, both of which allow seamless back-propagation by gradient descent. Coupled with the use of the cell based search, certain work has been able to drastically reduce the search complexity [16].

We make use of both the cell based search and gradient based search algorithms but propose a novel search space along with a modified cell template and a new regularized search objective to search binary networks.

2.3 Quantized Networks

In introduction, we mention that binary networks or 1-bit CNNs are distinguished from quantized networks (using more than 1 bit) and not fully binary networks (networks only with binary weights but floating point activations) due to the extreme memory savings and inference speed-up they bring. Quantized or not fully binarized networks that incorporate search are a type of efficient networks that are not comparable to 1-bit CNNs because they cannot utilize XNOR and bit counting operations in the inference which significantly brings down their memory savings and inference speed up gains.

It is, however, interesting to note that there are a line of work for efficient networks with more resource consumption, especially the recent ones. Notably, [57–60] search for multi-bit quantization policies only and solely [57] search for network architectures as well. [61] also search for network architectures for binary weight (not fully binarized) CNNs. Their networks are not fully binarized (networks only with binary weights) which makes them incomparable to other binary networks. Moreover, [58–60] all search for quantization policies, not network architectures, further differentiating it from our method.

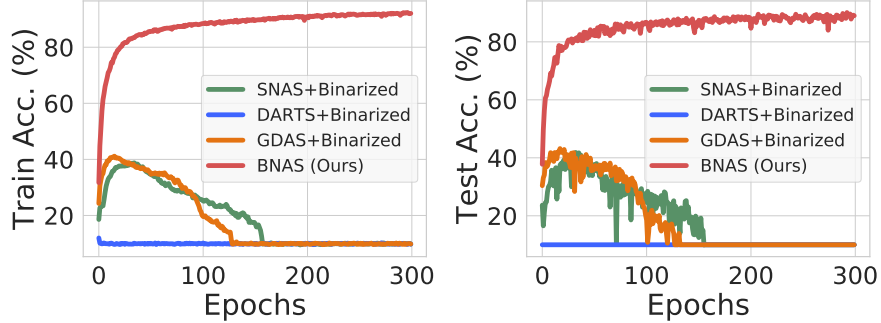


Figure 2: Train (left) and test (right) accuracy of binarized searched architectures on CIFAR10. The XNOR-Net’s binarization scheme and architectural modifications are applied in all cases. Contrasting to our BNAS, the binarized searched architectures fail to train well

3 Preliminary Study: Binarizing Searched Architectures by NAS

It is well known that architecture search results in better performing architecture than the hand-crafted ones. To obtain better binary networks, we first binarize the searched architectures by cell based gradient search methods. Specifically, we apply the binarization scheme of XNOR-Net along with their architectural modifications [7] to architectures searched by DARTS [14], SNAS [15] and GDAS [16]. We show the learning curves of the binarized searched floating point architectures on CIFAR10 dataset in Fig. 2.

Disappointingly, GDAS and SNAS reach around 40% test accuracy and quickly plummet while DARTS did not train at all. This implies that floating point NAS methods are not trivially extended to search binary networks. We investigate the failure modes in training and find two issues; 1) the search space is not well suited for binary networks, *e.g.*, using separable convolutions accumulates the quantization error repetitively and 2) the cell template does not propagate the gradients properly, due to quantization error. To search binary networks, the search space and the cell template should be redesigned to be robust to quantization error.

4 Approach

To search binary networks, we first write the problem of cell-based architecture search in general as:

$$\alpha^* = \operatorname{argmin}_{\alpha \in A(\mathcal{S}, T)} \mathcal{L}_S(D; \theta_\alpha), \quad (1)$$

where A is the feasible set of final architectures, \mathcal{S} is the search space (a set of layer types to be searched), T is the cell template which is used to create valid networks from the chosen layer types, \mathcal{L}_S is the search objective, D is the dataset, θ_α is the parameters of the searched architecture α which contain both architecture parameters (used in the continuous relaxation [14], Eq. 6) and the network weights (the learnable parameters of the layer types, Eq. 6), and α^* is the searched final architecture. Following [14], we solve the minimization problem using stochastic gradient descent (SGD).

Based on the observation in Sec. 3, we propose a new search space (\mathcal{S}_B), cell template (T_B) and a new search objective $\tilde{\mathcal{L}}_S$ for binary networks which have binary weights and activations. The new search space and the cell template are more robust to quantization error and the new search objective $\tilde{\mathcal{L}}_S$ promotes diverse search which is important when searching binary networks (Sec. 4.3). The problem of architecture search for binary network α_B^* can be rewritten as:

$$\alpha_B^* = \operatorname{argmin}_{\alpha_B \in A_B(\mathcal{S}_B, T_B)} \tilde{\mathcal{L}}_S(D; \theta_{\alpha_B}), \quad (2)$$

where A_B is the feasible set of binary network architectures and θ_{α_B} is parameters of the binary networks. We detail each proposal in the following subsections.

4.1 Search Space for Binary Networks (\mathcal{S}_B)

Unlike the search space used in floating point NAS, the search space used for binary networks should be robust to quantization error. Starting from the search space popularly used in floating point NAS [14–16, 39], we investigate the robustness of various convolutional layers to quantization error and selectively define the space for the binary networks. Note that the quantization error depends on the binarization scheme and we use the scheme proposed in [7].

Table 1: Test accuracy (%) of a small CNN composed of each layer type only, in floating point (FP Acc.) and in binary domain (Bin. Acc) on CIFAR10. *Conv*, *Dil. Conv* and *Sep. Conv* refer to the convolutions, dilated convolutions and separable convolutions, respectively. Separable convolutions show a drastically low performance on the binary domain

Layer Type Kernel Size	Conv		Dil. Conv		Sep. Conv	
	3 × 3	5 × 5	3 × 3	5 × 5	3 × 3	5 × 5
FP Acc. (%)	61.78	60.14	56.97	55.17	56.38	57.00
Bin. Acc. (%)	46.15	42.53	41.02	37.68	10.00	10.00

4.1.1 Convolutions and Dilated Convolutions

To investigate the various convolutional layers’ resilience to quantization error, we review the binarization scheme we use [7]. Let \mathbf{W} be the weights of a floating point convolution layer with dimension $c \cdot w \cdot h$ (number of channels, width and height of an input) and \mathbf{A} be an input activation. The floating point convolution can be approximated by binary parameters, \mathbf{B} , and the binary input activation, \mathbf{I} as:

$$\mathbf{W} * \mathbf{A} \approx \beta \mathbf{K} \odot (\mathbf{B} * \mathbf{I}), \quad (3)$$

where $*$ denotes the convolution operation, \odot is the Hadamard product (element wise multiplication), $\mathbf{B} = \text{sign}(\mathbf{W})$, $\mathbf{I} = \text{sign}(\mathbf{A})$, $\beta = \frac{1}{n} \|\mathbf{W}\|_1$ with $n = c \cdot w \cdot h$, $\mathbf{K} = \mathbf{D} * \mathbf{k}$, $\mathbf{D} = \frac{\sum |A_{i,:}|}{c}$ and $\mathbf{k}_{ij} = \frac{1}{w \cdot h} \forall ij$. Dilated convolutions are identical to convolutions in terms of quantization error as its only difference to ordinary convolution is the stride of convolution operations.

Since both convolutions and dilated convolutions show tolerable quantization error in binary networks [7] (and our empirical study in Table 1), we include the standard convolutions and dilated convolutions in our search space.

4.1.2 Separable Convolutions

Separable convolutions [62] have been widely used to construct efficient network architectures for floating point networks [4] in both hand-crafted and NAS methods. Unlike floating point networks, we argue that the separable convolution is not suitable for binary networks due to large quantization error. It uses nested convolutions to approximate a single convolution for computational efficiency. The nested convolution are approximated to binary convolutions as:

$$\begin{aligned} \text{Sep}(\mathbf{W} * \mathbf{A}) &\approx \beta_2 (\mathbf{B}_2 * \mathbf{A}_2) \\ &\approx \beta_1 \beta_2 (\mathbf{B}_2 * (\mathbf{K}_1 \odot (\mathbf{B}_1 * \mathbf{I}_1))), \end{aligned} \quad (4)$$

where $\text{Sep}(\mathbf{W} * \mathbf{A})$ denotes the separable convolution, \mathbf{B}_1 and \mathbf{B}_2 are the binary weights for the first and second convolution operation in the separable convolution layer, $\mathbf{I}_1 = \text{sign}(\mathbf{A})$, $\mathbf{A}_2 = \beta_1 \mathbf{K}_1 \odot (\mathbf{B}_1 * \mathbf{I}_1)$ and $\beta_1, \beta_2, \mathbf{K}_1$ are the scaling factors for their respective binary weights and activations. Since every scaling factor induces quantization error, the nested convolutions in separable convolutions will result in more (squared) quantization error.

To empirically investigate how the quantization error affects training for different convolutional layer types, we construct small networks formed by repeating each kind of convolutional layers three times, followed by three fully connected layers. We train these networks on CIFAR10 in floating point and binary domain and summarize the results in Table 1. When binarized, both convolution and dilated convolution layers show only a reasonable drop in accuracy, while the separable convolution layers show performance equivalent to random guessing (10% for CIFAR10). The observations in Table 1 imply that the accumulated quantization error by the nested convolutions fails binary networks in training. As DARTS [14] selects a large number of separable convolutions, it partly explains why the binarized architecture searched by DARTS in Fig. 2 does not train.

4.1.3 Zeroise

The *Zeroise* layer outputs all zeros irrespective of the input [14]. It was originally proposed to model the lack of connections. Further, in the authors’ implementation of [14]¹, the final architecture excludes the *Zeroise* layers and replaces it with the second best layer type, even if the search picks the *Zeroise* layers. Thus, the *Zeroise* layers are not being used as they were originally proposed but simply used as a placeholder for a different and sub-optimal layer type. Such replacement of layer types effectively removes all architectures that have *Zeroise* layers from the feasible set of final architectures.

¹<https://github.com/quark0/darts>

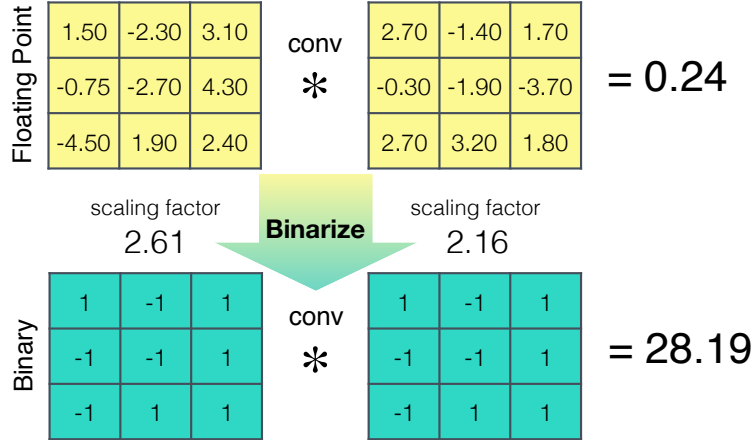


Figure 3: An example when the *Zeroise* layer is beneficial for binary networks. Since the floating point convolution is close to zero but the binarized convolution is far greater than 0, if the search selects the *Zeroise* layer instead of the convolution layer, the quantization error reduces significantly

Table 2: DARTS and BNAS w/ and w/o the *Zeroise* layers in the final architecture on CIFAR10. *Zeroise Layer* indicates whether the *Zeroise* layers were kept (✓) or not (✗). The test accuracy of DARTS drops by 3.02% when you include the *Zeroise* layers and the train accuracy drops by 63.54% and the training stagnates. In contrast, the *Zeroise* layers improves BNAS in both train and test accuracy

Precision	Floating Point (DARTS)			Binary (BNAS)		
	✗	✓	Gain	✗	✓	Gain
Including <i>Zeroise</i>	✗	✓	Gain	✗	✓	Gain
Train Acc. (%)	99.18	35.64	-63.54%	93.41	97.46	+4.05%
Test Acc. (%)	97.45	94.43	-3.02%	89.47	92.70	+3.23%

In contrast, we use the *Zeroise* layer for *reducing the quantization error* and first propose to keep it in the *final* architectures instead of using it as a placeholder for other layer types. As a result, our feasible set is different from that of [14] not only in terms of precision (binary), but also in terms of the network topology it contains.

As the exclusion of the *Zeroise* layers is not discussed in [14], we compare the accuracy with and without the *Zeroise* layer for DARTS in the ‘DARTS’ column of Table 2 and empirically verify that the *Zeroise* layer is not particularly useful for floating point networks. However, we observe that the *Zeroise* layer improve the accuracy by a meaningful margin in binary networks as shown in the table. We argue that the *Zeroise* layer can reduce quantization error in binary networks as an example in Fig. 3. Including the *Zeroise* layer in the final architecture is particularly beneficial when the situation similar to Fig. 3 happens frequently as the quantization error reduction is significant. But the degree of benefit may differ from dataset to dataset. As the dataset used for search may differ from the dataset used to train and evaluate the searched architecture, we propose to tune the probability of including the *Zeroise* layer. Specifically, we propose a generalized layer selection criterion to adjust the probability of including the *Zeroise* layer by a transferability hyper-parameter γ as:

$$p^* = \max \left[\frac{p_z}{\gamma}, p_{op_1}, \dots, p_{op_n} \right], \quad (5)$$

where p_z is the architecture parameter corresponding to the *Zeroise* layer and p_{op_i} are the architecture parameters corresponding to the i^{th} layer other than *Zeroise*. Larger γ encourages to pick the *Zeroise* layer only if it is substantially better than the other layers.

4.1.4 Final Search Space

With the separable convolutions and the *Zeroise* layer type considered, we summarize the defined search space for BNAS (\mathcal{S}_B) in Table 3.

Table 3: Proposed search space for BNAS. *Bin Conv*, *Bin Dil. Conv*, *Conv*, *MaxPool* and *AvgPool* refer to the binary convolution, binary dilated convolution, max pooling and average pooling layers, respectively

Layer Type	Bin Conv.		Bin Dil. Conv.		MaxPool	AvgPool	Zeroise
Kernel Size	3×3	5×5	3×3	5×5	3×3	3×3	N/A

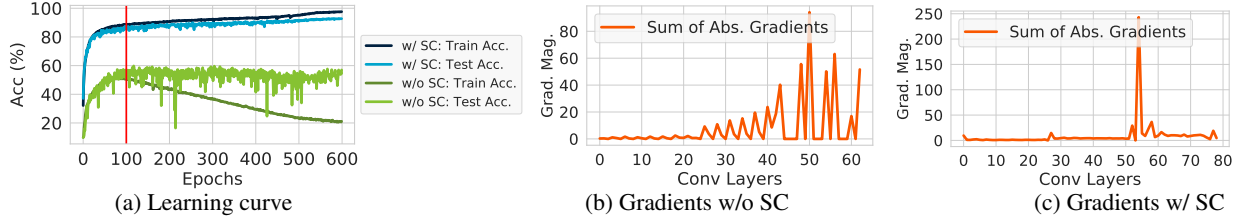


Figure 4: Unstable gradients in the binary domain. ‘w/o SC’ indicates the cell template of [39] (Fig. 5-(a)). ‘w/ SC’ indicates the proposed cell template (Fig. 5-(b)). The gradient magnitudes are taken at epoch 100. With the proposed cell template (‘w/ SC’), the searched network trains well (a). The proposed cell template shows far less spiky gradients along with generally larger gradient magnitudes ((b) vs. (c)), indicating that our template helps to propagate gradients more effectively in the binary domain

4.2 Cell Template for Binary Networks (T_B)

With the defined search space, we now learn a network architecture with the convolutional cell template proposed in [39]. However, the learned architecture still suffers from unstable gradients in the binary domain as shown in Fig. 4-(a) and (b). Investigating the reasons for the unstable gradients, we observe that the skip-connections in the cell template proposed in [39] are confined to be inside a single convolutional cell, *i.e.*, intra-cell skip-connections. The intra-cell skip-connections do not propagate the gradients outside the cell, forcing the cell to aggregate outputs that always have quantization error created inside the cell. To help convey information without the cumulative quantization error through multiple cells, we propose to add skip-connections between multiple cells as illustrated in Fig. 5.

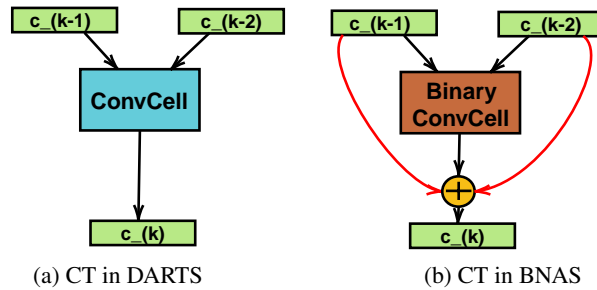


Figure 5: Cell templates (CT) of (a) DARTS and (b) BNAS. Red lines in BNAS indicate inter-cell skip connections. ConvCell indicates the convolutional cell. $c_{(k)}$ indicates the output of the k^{th} cell

The proposed cell template with inter-cell skip-connections help propagate gradients with less quantization error throughout the network, stabilizing the training curve. We empirically validate the usefulness of the inter-cell skip connections in Sec. 6.5.

4.3 Search Objective with Diversity Regularizer ($\tilde{\mathcal{L}}_S$)

With the feasible set of binary architectures (A_B) defined by S_B and T_B , we solve the optimization problem similar to [14]. However, the layers with learnable parameters (*e.g.*, convolutional layers) are not selected as often early on as the layers requiring no learning, because the parameter-free layers are more favorable than the under-trained layers. The problem is more prominent in the binary domain because binary layers train slower than the floating point counterparts [20]. To alleviate this, we propose to use an exponentially annealed entropy based regularizer in the search objective to promote selecting diverse layers and call it the *diversity regularizer*. Specifically, we subtract the entropy of the architecture parameter distribution from the search objective as:

$$\tilde{\mathcal{L}}_S(D; \theta_{\alpha_B}) = \mathcal{L}_S(D; \theta, p) - \lambda H(p) e^{(-t/\tau)}, \quad (6)$$

Table 4: Effect of searching diversity on CIFAR10. *Diversity* refers to whether diversity regularization was applied (✓) or not (✗) during the search. DARTS only gains 0.20% test accuracy while BNAS gains 1.75% test accuracy

Precision Diversity	Floating Point (DARTS)			Binary (BNAS)		
	✗	✓	Gain	✗	✓	Gain
Test Acc. (%)	96.53	96.73	+0.20	90.95	92.70	+1.75

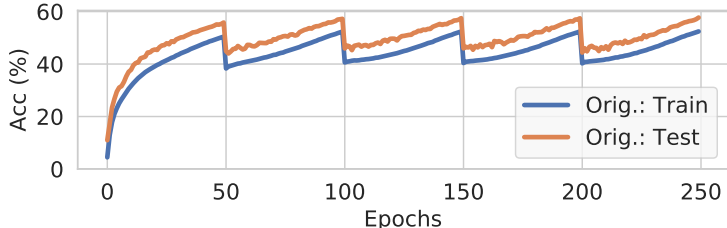


Figure 6: Training curve for vanilla training scheme [31] on ImageNet. Notice that the training accuracy is lower than the test accuracy indicating an underfitting problem, rather than an overfitting problem as is commonly seen in neural network training.

where $\mathcal{L}_S(\cdot)$ is the search objective of [14], which is a cross-entropy, θ_{α_B} is the parameters of the sampled binary architecture, which is split into the architecture parameters p and the network weights θ , $H(\cdot)$ is the entropy, λ is a balancing hyper-parameter, t is the epoch, and τ is an annealing hyper-parameter. This will encourage the architecture parameter distribution to be closer to uniform in the early stages, allowing the search to explore diverse layer types.

Using the proposed diversity regularizer, we observed a 16% relative increase in the average number of learnable layer types selected in the first 20 epochs of the search. More importantly, we empirically validate the benefit of the diversity regularizer with the test accuracy on the CIFAR10 dataset in Table 4 and in Sec. 6.5. While the accuracy improvement from the diversity regularizer in the floating point NAS methods such as DARTS [14] is marginal (+0.2%), the improvement in our binary network is more meaningful (+1.75%).

5 Training the Searched Architectures

While our main focus is on searching better architectures for binary networks, it is of orthogonal interest to find a better training scheme for our searched architectures. Given that most recent works on binary networks that propose novel training methods or regularizers [17, 18, 38] report their results for binary networks with floating point architectures like the ResNet18 or AlexNet, it is interesting to investigate a training method for the searched architectures for binary networks.

5.1 Stochastic Gradient Descent with Cosine Annealing

We first use the standard training procedure of using the stochastic gradient descent (SGD) optimizer with weight decay along with a cosine annealing restart learning rate scheduler. We also used the standard data augmentation including horizontal flipping and color jittering. Fig. 6 shows a training curve of our searched architectures on the ImageNet dataset. The sudden drops in accuracy correspond to the epochs when the learning rate scheduler is warmly restarted *i.e.*, when the learning rate is reset to the initial (and larger) value. Note that while the accuracy increase as the epochs progress, the training accuracy is consistently below the test accuracy. While one could argue that this indicates good generalization capability, by the observation that the test accuracy is not high enough ($\sim 60\%$), we hypothesize that this may be an indication of an underfitting.

This phenomenon has never been analyzed with the binary networks in the literature as of today. We suspect that our searched architectures may be able to encode inputs better and have yet to fit the training set because of the excess regularization present in the standard training scheme. Hence, we hypothesize that regularization may actually not help in training our searched architectures.

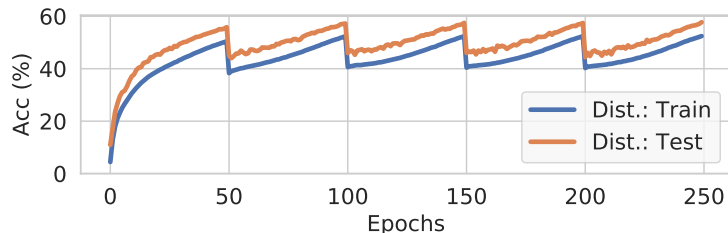


Figure 7: Training curve for the activation distribution regularizer on ImageNet. Notice that the training accuracy is still lower than the test accuracy indicating an underfitting problem and that the regularizer does not help to combat this trend

5.2 Regularization for Training Our Searched Architectures

To investigate our hypothesis, we consider recently proposed regularizers [17, 18] for training binary networks. Activation distribution [17] regularizes the training under the assumption that $+1$ and -1 are equally likely in a binary network. [18] also uses a similar assumption to [17] and regularizes the network indirectly by their Libra binarization scheme. To clearly verify our hypothesis that regularization may actually not help in training our searched architectures, we use a direct regularizer [17]. Thus, we use the activation distribution regularizer and show the training curve on the ImageNet dataset in Fig. 7. We observe that the regularizer results in similar learning curve to Fig. 6 where the train accuracy is constantly lagging behind the test accuracy. In addition, the use of the regularizer costs additional computation. By the above empirical studies, we conjecture that training our searched architectures may need better fitting to the dataset instead of using excess regularization.

5.2.1 Minimal Regularization

Recently, advances in training deep neural networks have resulted in models that almost always fit well to the training data. In other words, the need to address the underfitting problem (*i.e.*, large bias in the bias-variance trade-off) in the floating point deep neural network literature have been greatly reduced. In line with the observed trends, there are a number of recent works on binary networks that also focused on improving the generalization of binary networks via various regularization techniques [17, 18]. However, as binary networks have extremely reduced capacity compared to their floating point counterparts, we argue that binary networks must first be trained to better fit to the training data. We here propose to not use the regularization techniques proposed by [17, 18] as well as other more commonly used techniques such as weight decay and color jittering and call this training scheme the *minimal regularization scheme*. We also use the simpler cosine annealing learning rate scheduler without the warm restart.

In Fig. 8, we plot the training curve of our searched binary network with the proposed training method. We observe that the network has little underfitting problems along with better generalization *i.e.*, the training accuracy is slightly higher than the test accuracy and the test accuracy is noticeably improved. Compared to the conventional training scheme that use standard SGD with weight decay and cosine annealed restart learning scheduling, the proposed scheme achieves almost a $+4\%$ improvement in top-1 test accuracy and $+3\%$ in top-5 test accuracy on ImageNet. As such, going back to the basic idea of addressing the underfitting problem (*i.e.* reducing bias in the bias-variance tradeoff) in machine learning models can lead to great improvements.

Complementary to the minimal regularization training scheme, we found that using group convolutions for the layers that are not binarized in our binary networks, *i.e.*, the convolution layers in the stem of our net, and increasing the number of channels gives better accuracy without increases of FLOPs. Similar trends have also been found in [32]. As shown in Fig. 8, this further improves the test accuracy by around $+2\%$ for both top-1 and top-5 accuracy.

5.2.2 Minimal Regularization with Longer Training

As better fitting is of interest than regularizing training, we let model be trained with longer epochs and achieved higher accuracy. Training the model for longer epochs (250 to 500) improves accuracy by about $+1\%$ in both top-1 and top-5 metric on ImageNet as shown in Fig. 9.

We compare discussed training schemes in Fig. 10 to contrast the learning curves. We observe that the minimal regularization scheme shows clear gain compared to the standard SGD with weight decay. Note that to isolate the architectural gains from searching the architectures and the gains by the new training scheme, we separately present experimental results with standard SGD and with the proposed training schemes in Sec. 6.

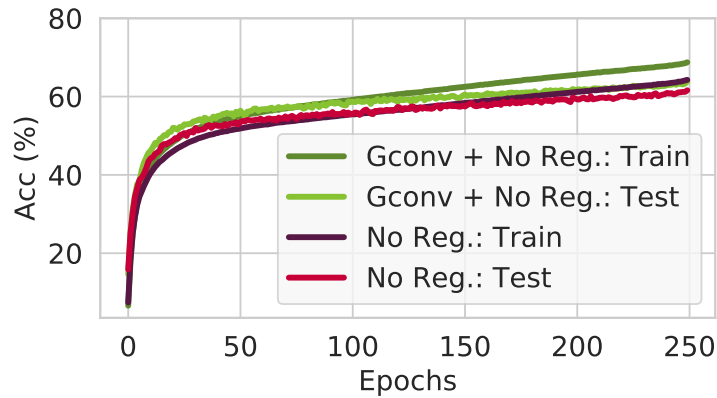


Figure 8: Training curve for minimal regularization on ImageNet. Notice that the training accuracy is slightly higher than the test accuracy and the underfitting problem is mitigated. Using group convolutions, the performance is further increased

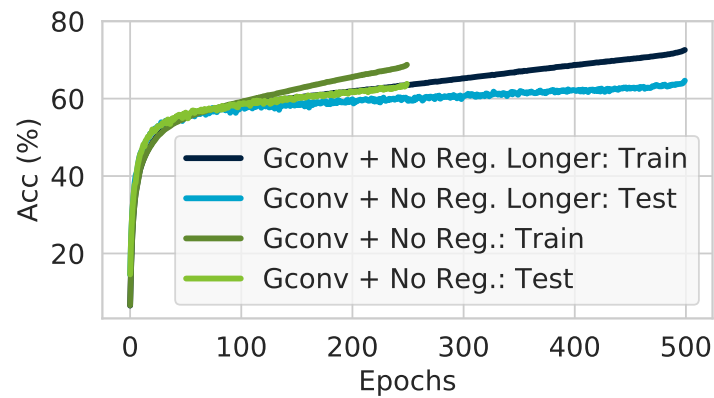


Figure 9: Training curve for minimal regularization including longer epochs on ImageNet. Training the model for longer, *i.e.* fitting better to the training data, increases the performance further

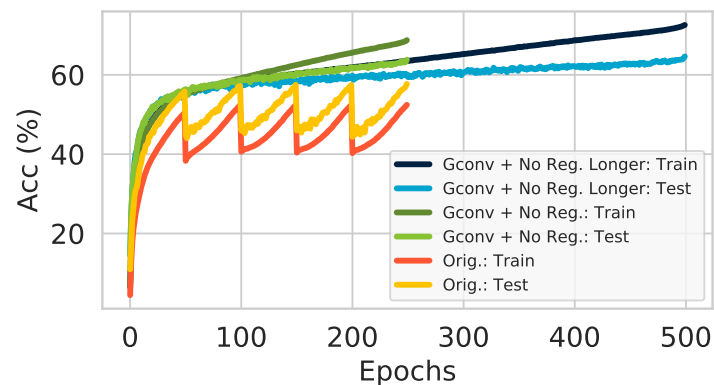


Figure 10: Comparison of training curves for various training schemes on ImageNet. The minimal regularization training scheme helps to increase the performance by mitigating the underfitting problem. Training the model longer further improves the final test accuracy

Table 5: Configuration details of BNAS variants. *# Cells*: the number of stacked cells. *# Chn.*: the number of output channels of the first convolution layer of the model. γ is the transferrability hyper-parameter in Eq. 5

BNAS-	Mini	A	B	C	D	E	F	G	H
# Cells	10	20	12	16	12	12	15	11	16
# Chn.	24	36	64	108	64	68	68	74	128
γ	1	1	1	1	3	3	3	3	3
Dataset	CIFAR10				ImageNet				

6 Experiments

6.1 Experimental Setup

Datasets. We use CIFAR10 [63] and ImageNet (ILSVRC 2012) [64] datasets to evaluate the image classification accuracy. For searching binary networks, we use the CIFAR10 dataset. For training the final architectures from scratch, we use both CIFAR10 and ImageNet. During the search, we hold out half of the training data of CIFAR10 as the validation set to evaluate the quality of search. For final evaluation of the searched architecture, we train it from the scratch using the full training set and report Top-1 (and Top-5 for ImageNet) accuracy.

Details on Searching Architectures. We train a small network with 8 cells and 16 initial number of channels using SGD with the diversity regularizer (Sec. 4.3) for 50 epochs with batch size of 64. We use momentum 0.9 with initial learning rate of 0.025 using cosine annealing [65] and a weight decay of 3×10^{-4} . We use the same architecture hyper-parameters as [14] except for the additional diversity regularizer where we use $\lambda = 1.0$ and $\tau = 7.7$. Our cell search takes approximately 4 hours on a single NVIDIA GeForce RTX 2080Ti GPU.

Details on Training the Searched Architectures. For the standard scheme, we train the models for 250 epochs with batch size 512. We use SGD with momentum 0.9, with an initial learning rate of 0.1 and a weight decay of 3×10^{-5} . We use the cosine annealing restart scheduler [65] with the minimum learning rate of 0 and the length of one cycle being 50 epochs.

For the minimal regularization scheme, we use the Adam optimizer with no weight decay and cosine annealing learning rate scheduler. We do not use color jittering for this scheme to minimize the regularization effect. We also train the model for 500 epochs for the longer training scheme.

For CIFAR10, we use the standard scheme only where we train the final networks for 600 epochs with batch size 256. We use SGD with momentum 0.9 and weight decay of 3×10^{-6} . We use the one cycle learning rate scheduler [66] with the learning rate ranging from 5×10^{-2} to 4×10^{-4} . For ImageNet, we use the standard SGD scheme and the minimal regularization scheme mentioned in Section 5.2.

Final Architecture Configurations. We vary the size of our BNAS to compare with the other binary networks with different FLOPs by stacking the searched cells and changing the output channels of the first convolutional layer and name them as BNAS-{Mini, A, B, C, D, E, F, G, H} as shown in Table 5.

Details on Comparison with Other Binary Networks. For XNOR-Net with different backbone architectures, we use the floating point architectures from `torchvision` or a public source² and apply the binarization scheme of XNOR-Net. Following previous work [11, 25] on comparing ABC-Net with a single base [22], we compare PCNN with a single projection kernel for both CIFAR10 and ImageNet. The code and learned models are available in our repository³.

6.2 Qualitative Analysis of the Searched Cell

We first qualitatively compare our searched cell with the XNOR-Net cell based on the ResNet18 architecture in Fig. 11. As shown in the figure, our searched cell has a contrasting structure to the handcrafted ResNet18 architecture. Both cells contain only two 3×3 binary convolution layer types, but the extra *Zeroise* layer types selected by our search algorithm help in reducing the quantization error. The topology in which the *Zeroise* layer types and convolution layer types are connected also contributes to improving the classification performance of our searched cell.

²<https://github.com/kuangliu/pytorch-cifar>

³<https://github.com/gistvision/bnas>

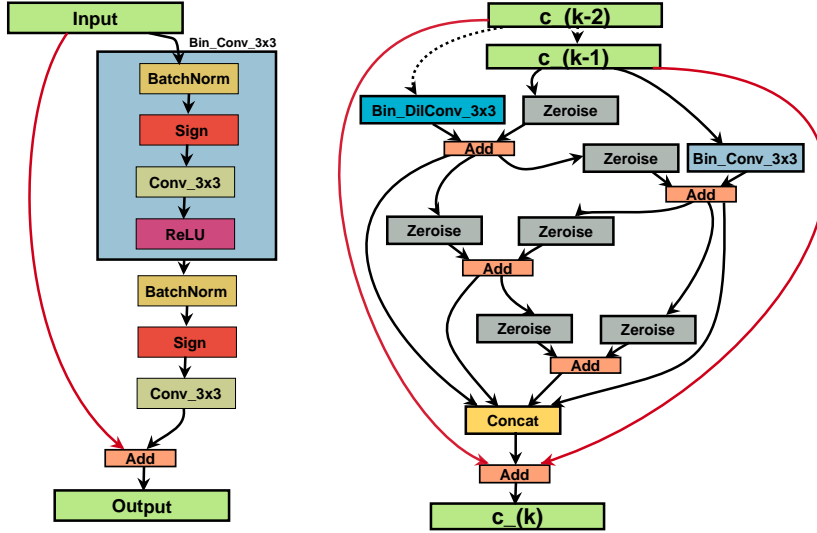


Figure 11: Comparing BNAS cell (right) to XNOR-Net cell (left). $c_{-}(k)$ denotes the output of the k^{th} cell. The dotted lines represents the connections from the second previous cell ($c_{-}(k-2)$). The red lines correspond to skip connections

We then conduct further qualitative analyses of both the normal cell and the reduction cell of our searched cell with the binarized DARTS cell [14].

Normal Cell. In Fig. 12-(a) and (c), we compare the normal cell of BNAS with the normal cell of DARTS [14]. Our cell has inter-cell skip connections which result in more stable gradients leading to better training, whereas the binarized DARTS cell does not train at all (achieving only 10.01% test accuracy on CIFAR10 in Fig. 2). We hypothesize that the lack of inter-cell skip connections in their cell template may also contribute to the failure of its architecture in the binary domain other than the excessive number of separable convolutions in the DARTS searched cell.

Reduction Cell. We also qualitatively compare the BNAS reduction cell to the binarized DARTS reduction cell in Figure 12-(b) and (d). Note that the BNAS reduction cell has a lot of *Zeroise* layers which help reduce quantization error.

In the following subsections, we show that our searched topology yields better binary networks that outperform the architectures used in state-of-the-art binary networks.

6.3 Quantitative Analysis

We now quantitatively compare our searched architectures to various binary networks.

6.3.1 Comparisons on Backbone Architectures for Binary Networks

We first compare our searched architectures to various backbone architectures that have been used in the state-of-the-art binary networks with the binarization scheme of XNOR-Net [7] in Table 6. We use the standard training scheme for this comparison. The comparisons differ only in the backbone architecture, allowing us to isolate the effect of our searched architectures on the final accuracy, *i.e.*, the comparison with XNOR-Net with different backbone architectures for various FLOPs and newer binary networks with the architectural contributions only. To single out the architectural contributions of Bi-Real Net, we used Table 1 in [11] to excerpt the ImageNet classification accuracy with using only the Bi-Real Net architecture. Note that CBCN is based on the Bi-Real Net architecture with the convolutions being changed to circulant convolutions⁴. Additionally, as mentioned in Sec. 2, we do not compare with [13] as the inference speed-up is significantly worse than other binary networks ($\sim 2.7\times$ compared to $\sim 10\times$), which makes the comparison less meaningful.

As shown in Table 6, our searched architectures outperform other architectures used in binary networks in all FLOPs brackets and on both CIFAR10 and ImageNet. Notably, comparing XNOR-Net with the ResNet18 and ResNet34

⁴They mention that center loss and gaussian gradient update is also used but they are not elaborated and not the main focus of CBCN’s method.

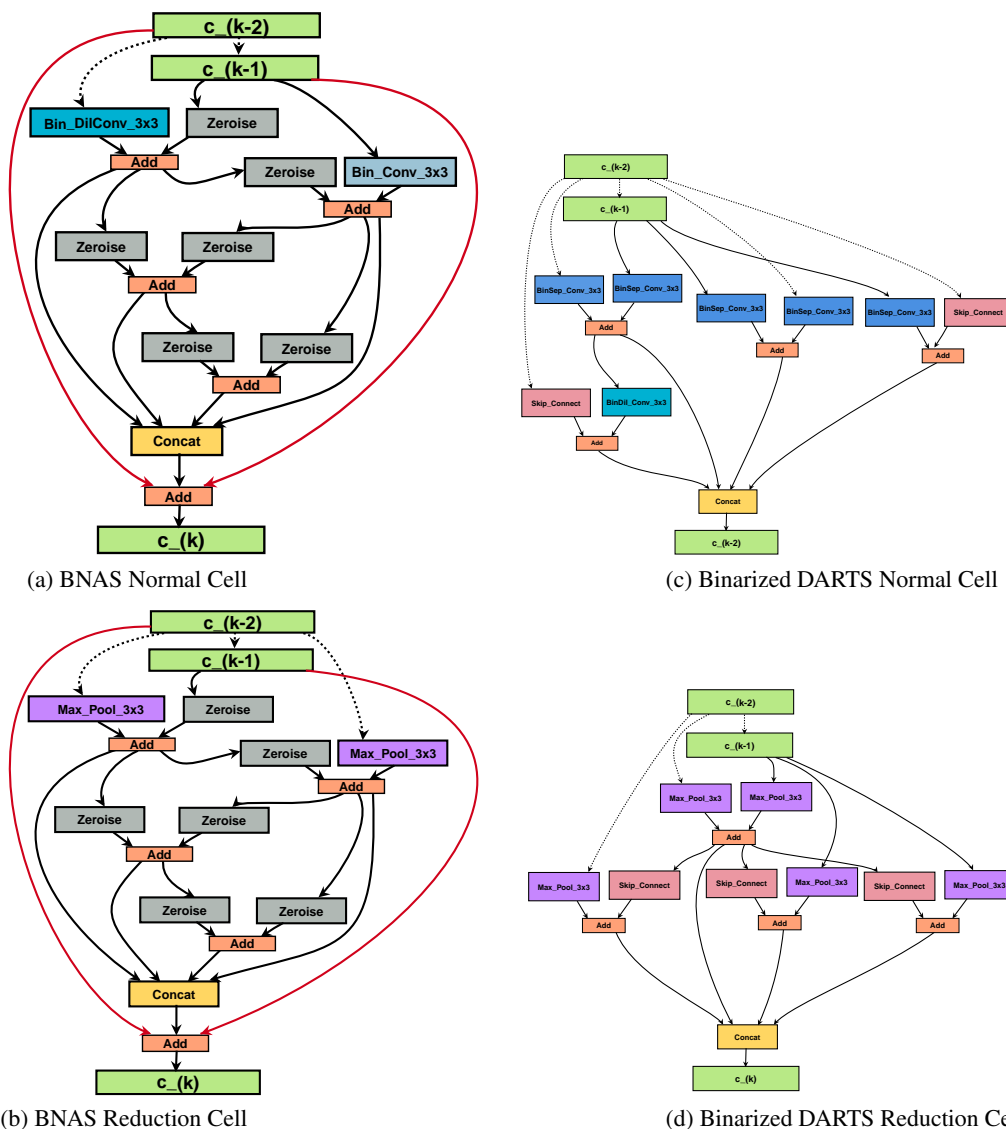


Figure 12: Comparing the normal and reduction cell of BNAS (a)-(b) and those of binarized DARTS (c)-(d). $c_{(k)}$ indicates the output of the k^{th} cell. The dotted lines represent the connections from the second previous cell ($c_{(k-2)}$). **Red lines** in (a)-(b) indicate the inter-cell skip connections. Note that the searched cell of binarized DARTS has only intra-cell skip connections (denoted by pink boxes) which have unstable gradients as compared to inter-cell skip connections BNAS cells (See discussions in Section 4.2). Interestingly, the BNAS reduction cell only uses the output from the second previous cell ($c_{(k-2)}$) as inputs to the max pool layers, utilizing the inter-cell skip connections more

backbone to BNAS-D and BNAS-F, we gain +6.49% or +2.50% top-1 accuracy and +6.69% or +1.72% top-5 accuracy on ImageNet.

Furthermore, BNAS retains the accuracy much better at lower FLOPs, showing that our searched architectures are better suited for efficient binary networks. Additionally, comparing CBCN to BNAS-H, we gain +2.11% top-1 accuracy and +1.11% top-5 accuracy, showing that our architecture can scale to higher FLOPs budgets better than CBCN. In sum, replacing the architectures used in current binary networks to our searched architectures can greatly improve the performance of binary networks.

Table 6: Comparison of different backbone architectures for binary networks with XNOR-Net binarization scheme [7] in various FLOPs budgets. Bi-Real* indicates Bi-Real Net’s method with only the architectural modifications. We refer to [37] for the FLOPs of CBCN. CBCN* indicates the highest accuracy for CBCN with the ResNet18 backbone as [12] report multiple different accuracy for the same network configuration. Additionally, [12] does not report the exact FLOPs of their model, hence we categorized them conservatively into the ‘ ~ 0.27 ’ bracket

Dataset	FLOPs ($\times 10^8$)	Model (Backbone Arch.)	Top-1 Acc. (%)	Top-5 Acc. (%)
CIFAR10	~ 0.16	XNOR-Net (ResNet18)	88.82	-
		XNOR-Net (DenseNet)	85.16	-
		XNOR-Net (NiN)	86.28	-
		XNOR-Net (SENet)	88.12	-
		BNAS-A	92.70	-
	~ 0.27	XNOR-Net (ResNet34)	88.54	-
		XNOR-Net (WRN40)	91.58	-
		CBCN* (ResNet18) [12]	91.91	-
		BNAS-B	93.76	-
	~ 0.90	XNOR-Net (ResNext29-64)	84.27	-
		BNAS-C	94.43	-
	ImageNet	~ 1.48	XNOR-Net (ResNet18)	51.20
BNAS-D			57.69	79.89
~ 1.63		Bi-Real* (Bi-Real Net18) [11]	32.90	56.70
		BNAS-E	58.76	80.61
~ 1.78		XNOR-Net (ResNet34)	56.49	79.13
		BNAS-F	58.99	80.85
~ 1.93		Bi-Real* (Bi-Real Net34) [11]	53.10	76.90
		BNAS-G	59.81	81.61
~ 6.56	CBCN (Bi-Real Net18) [12]	61.40	82.80	
	BNAS-H	63.51	83.91	

6.3.2 Comparison with Other Binary Networks

To compare the gains from the architectural changes to gains from other methods for learning binary networks in the literature, we compare our searched architectures to various state-of-the-art binary networks. We first use the standard training scheme to isolate the gains from architectural improvements.

As shown in Table 7, our searched architectures outperform other methods in more than half the FLOPs brackets spread across CIFAR10 and ImageNet. Moreover, the state-of-the-art methods that focus on discovering better training schemes are complementary to our searched architectures, as these training methods were not designed exclusively for a fixed network topology.

Note that, with the same backbone of ResNet18 or ResNet34, Bi-Real, PCNN, XNOR-Net++ and BONN have higher FLOPs than ABC-Net, XNOR-Net and BinaryNet. The higher FLOPs are from unbinarizing the downsampling convolutions in the ResNet architecture.⁵

6.4 BNAS using the Minimal Regularization Training Scheme

We also compare our searched architecture trained with the minimal regularization training scheme to other binary networks with their own best training methods on the ImageNet dataset in Table 8. Note that with much smaller FLOPs and no pretraining scheme, BNAS-D-No-Reg is able to achieve noticeably high accuracy, slightly worse than Bi-Real (Bi-Real Net34) which uses 30% more FLOPs. More importantly, BNAS-D-No-Reg[†] improves over BNAS-D-No-Reg by over 2% top-1 accuracy, achieving the second highest accuracy amongst the compared networks with the lowest FLOPs. Finally, BNAS-D-No-Reg-Longer[†] achieves the state-of-the-art accuracy, indicating that fitting better to the training set via an extended training is beneficial.

⁵We have confirmed with the authors of [7] that their results were reported without unbinarizing the downsampling convolutions.

Table 7: Comparison of other binary networks in various FLOPs budgets. The binarization schemes are: ‘*Sign + Scale*’: using fixed scaling factor and the sign function [7], ‘*Sign*’: using the sign function [20], ‘*Clip + Scale*’: using clip function with shift parameter [22], , ‘*Sign + Scale**’: using learned scaling factor and the sign function [26], ‘*Projection*’: using projection convolutions [25], ‘*Bayesian*’: using a learned scaling factor from the Bayesian losses [34] and the sign function, and ‘*Decoupled*’: decoupling ternary activations to binary activations [37]

Dataset	FLOPs ($\times 10^8$)	Method (Backbone Arch.)	Binarization Scheme	Pretraining	Top-1 Acc. (%)	Top-5 Acc. (%)
CIFAR10	~ 0.04	PCNN($i = 16$) (ResNet18) [25]	Projection	✗	89.16	-
		BNAS-Mini	Sign + Scale	✗	90.12	-
	~ 0.16	BinaryNet (ResNet18) [20]	Sign	✗	89.95	-
		BNAS-A	Sign + Scale	✗	92.70	-
	~ 0.27	PCNN($i = 64$) (ResNet18) [25]	Projection	✓	94.31	-
		BNAS-B	Sign + Scale	✗	93.76	-
ImageNet	~ 1.48	BinaryNet (ResNet18) [20]	Sign	✗	42.20	67.10
		ABC-Net (ResNet18) [22]	Clip + Sign	✗	42.70	67.60
		BNAS-D	Sign + Scale	✗	57.69	79.89
	~ 1.63	Bi-Real (Bi-Real Net18) [11]	Sign + Scale	✓	56.40	79.50
		XNOR-Net++ (ResNet18) [26]	Sign + Scale*	✗	57.10	79.90
		PCNN (ResNet18) [25]	Projection	✓	57.30	80.00
		BONN (Bi-Real Net18) [34]	Bayesian	✗	59.30	81.60
		BinaryDuo (ResNet18) [37]	Decoupled	✓	60.40	82.30
		BNAS-E	Sign + Scale	✗	58.76	80.61
	~ 1.78	ABC-Net (ResNet34) [22]	Clip + Scale	✗	52.40	76.50
		BNAS-F	Sign+Scale	✗	58.99	80.85
	~ 1.93	Bi-Real (Bi-Real Net34) [11]	Sign + Scale	✓	62.20	83.90
		BNAS-G	Sign + Scale	✗	59.81	81.61

Table 8: Comparison of other binary networks with our architectures using the minimal regularization scheme. Our architectures with various training schemes are indicated by gray cells. Models with the † symbol indicates using group convolutions at the non-binary layers, as mentioned in Section 5.2. Note that our BNAS-D model that has the smallest FLOPs budget outperforms all other state-of-the-art binary networks with larger FLOPs budgets by non trivial margins and achieve state-of-the-art accuracy by a binary network.

Dataset	FLOPs ($\times 10^8$)	Method (Backbone Arch.)	Binarization Scheme	Pretraining	Top-1 Acc. (%)	Top-5 Acc. (%)
ImageNet	~ 1.48	BinaryNet (ResNet18) [20]	Sign	✗	42.20	67.10
		ABC-Net (ResNet18) [22]	Clip + Sign	✗	42.70	67.60
		BNAS-D	Sign + Scale	✗	57.69	79.89
		BNAS-D-No-Reg	Sign + Scale	✗	61.60	82.91
		BNAS-D-No-Reg [†]	Sign + Scale	✗	63.82	84.25
		BNAS-D-No-Reg-Longer [†]	Sign + Scale	✗	64.63	84.90
	~ 1.63	Bi-Real (Bi-Real Net18) [11]	Sign + Scale	✓	56.40	79.50
		XNOR-Net++ (ResNet18) [26]	Sign + Scale*	✗	57.10	79.90
		PCNN (ResNet18) [25]	Projection	✓	57.30	80.00
		BONN (Bi-Real Net18) [34]	Bayesian	✗	59.30	81.60
		BinaryDuo (ResNet18) [37]	Decoupled	✓	60.40	82.30
	~ 1.78	ABC-Net (ResNet34) [22]	Clip + Scale	✗	52.40	76.50
	~ 1.93	Bi-Real (Bi-Real Net34) [11]	Sign + Scale	✓	62.20	83.90
	~ 6.56	CBCN (Bi-Real Net18) [12]	Sign + Scale	✓	61.40	82.80

Comparing the above two results with BNAS-D, which uses the standard training scheme, we can see that there is a lot of room to improve by simply fitting well to the training data. Hence, contrary to recent research directions in binary networks which involves new regularizations, we argue that a binary network with better architecture needs to fit to the training data more.

6.4.1 Comparison to recent searched binary network - BATS [32]

BATS [32] is a very recent, concurrent to our previous conference version, which also aims to search binary networks. Note that there are several differences in how BATS searches their architectures compared to ours such as the search space, the search objective, and the extent to which the networks are binarized. In addition to the differences during the search phase, there are significant differences in how BATS trains their architectures. Although it is seldom described in

their paper, we have confirmed with the authors that they use a non-trivial multi-stage training scheme similar to [38]. The training requires three additional networks to be trained sequentially beforehand and involves techniques similar to attention transfer [67] and pretraining. Therefore, the performance of the reported BATS architecture is a composite function of better architecture and their non-trivial training method.

To provide clearer insight on the comparative advantage of the architectures searched by our method, we compare the top-1 and top-5 accuracy of the searched architectures with various training schemes including the one used in BATS [32] in Table 9. Note that BNAS-D[†] (it is a BNAS-D model with the group convolutions as explained in Sec. 5.2.1) achieves comparable performance to the BATS architecture when the BATS multi-stage training scheme is used. However, when trained with the more conventional SGD with the cosine annealing or with our ‘minimal regularization’ training scheme, our architecture outperforms the BATS architecture by large margins. Interestingly, the final accuracy of the BATS architecture heavily varies depending on how much regularization was used during training whereas BNAS-D[†] does not vary as much. In addition, BATS searches their architecture in a non-binary (floating point weights and binary activation) domain while we search architectures in a fully binarized domain. Hence, the gap between the search phase and the training phase is larger in BATS than ours, thus BATS may require more regularization to train properly.

In terms of computational efficiency, the multi-stage training of BATS [32, 38] took up to $8\times$ more training time than our ‘minimal regularization’ training scheme due to the additional pretraining stage and the extra complexity from using attention transfer. There are also more hyperparameters (*e.g.*, the temperature and weighting hyperparameter) to tune which leads to more variance and less reproducibility. In contrast, our training scheme simply requires the network to be trained with less regularization, which leads to remarkable improvements despite the simplicity of the method.

Table 9: Comparison with BATS on various training schemes. ‘SGD w/ Cosine annealing’ refers to the standard training method described in Section 5.1. ‘Minimal Regularization’ refers to our minimal regularization training scheme described in Section 5.2.1. ‘BATS multi-stage’ refers to the training scheme used by BATS similar to [38]. * indicates that the result was excerpted from [32]

Training Method	BNAS-D [†]	BATS [32]
SGD w/ Cosine annealing	57.69% / 79.89%	52.97% / 76.99%
Minimal Regularization	63.82% / 84.25%	38.76% / 63.65%
BATS multi-stage [32, 38]	66.03% / 85.42%	66.10%* / 87.00%*

6.5 Ablation Studies

We perform ablation studies on the proposed components of our method. We use the CIFAR10 dataset for the experiments with various FLOPs budgets and summarize the results in Table 10. All components have decent contributions to the accuracy, with the inter-cell skip connection in the new cell template contributing the most; without it, the models eventually collapsed to very low training and test accuracy and exhibited unstable gradient issues as discussed in Sec. 4.2. Comparing *No Div* with *Full*, the searched cell with the diversity regularizer has a clear gain over the searched cell without it in all the model variants. Interestingly, the largest model (BNAS-C) without *Zeroise* layers performs worse than BNAS-A and BNAS-B, due to excess complexity.

6.5.1 ‘No Skip’ Setting

Besides the final classification accuracy presented in Table 10, here we additionally present the train and test accuracy curves for the *No Skip* ablation models of Table 10 in Fig. 13 for more detailed analysis. All three variants collapse to a very low training and test accuracy after a reasonable number of epochs (600).

In Fig. 14, which shows the gradients of the ablated models at epoch 100 similar to Figure 4, we again observe that the ablated BNAS- $\{A,B,C\}$ without the inter-cell skip connections have unstable (spiky) gradients. We additionally provide temporally animated plots of the gradients to demonstrate how they change at every 10 epochs starting from 100 epoch to 600 epoch in the accompanied mp4 file – ‘comb_grads.mp4’ as a supplementary material. Table 11 shows the details of the plots in the ‘comb_grads.mp4’ file.

Note that the ablated models (‘BNAS-A w/o SC’, ‘BNAS-B w/o SC’ and ‘BNAS-C w/o SC’) have unstable (spiky) gradients in the early epochs while the full model (‘BNAS-A w/ SC’) shows relatively stable (less spiky) gradients in all epochs. All models eventually show small gradients, indicating the models have stopped learning. However, while the training curve of the full model (Figure 4) implies that it has converged to a reasonable local optima, the training curves of the ablated models (Figure 13) imply that they converged to a poor local optima instead.

Table 10: Classification acc. (%) of ablated models on CIFAR10. *Full* refers to the proposed method with all components. *No Skip*, *No Zeroise*, and *No Div* refers to our method without the inter-cell skip connections, with explicitly discarding the *Zeroise* layers, or without the diversity regularizer, respectively.

Model	Full	No Skip	No Zeroise	No Div
BNAS-A	92.70	61.23	89.47	90.95
BNAS-B	93.76	67.15	91.69	91.55
BNAS-C	94.43	70.58	88.74	92.66

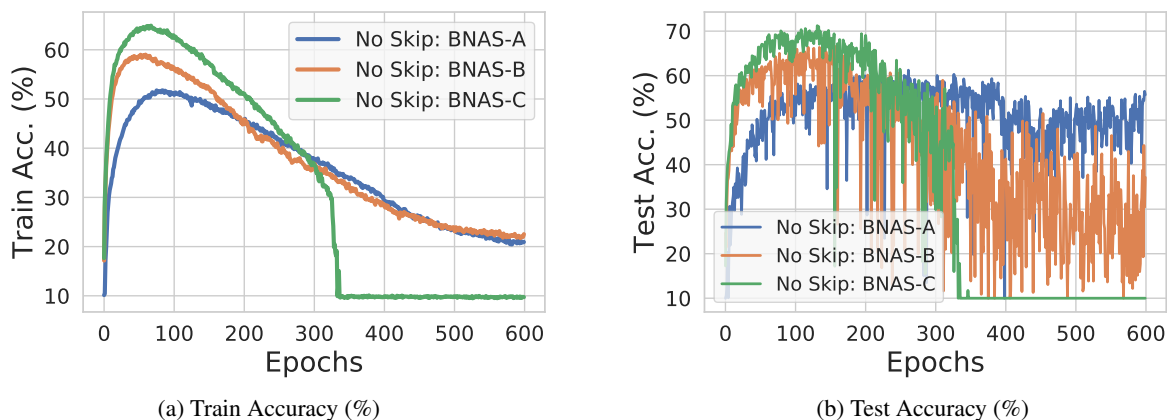


Figure 13: Learning curve for the ‘No Skip’ ablation on CIFAR10. The train (a) and test (b) accuracy of all three models collapse when trained for 600 epochs. Additionally, the test accuracy curves fluctuates heavily when compared to the train accuracy curve

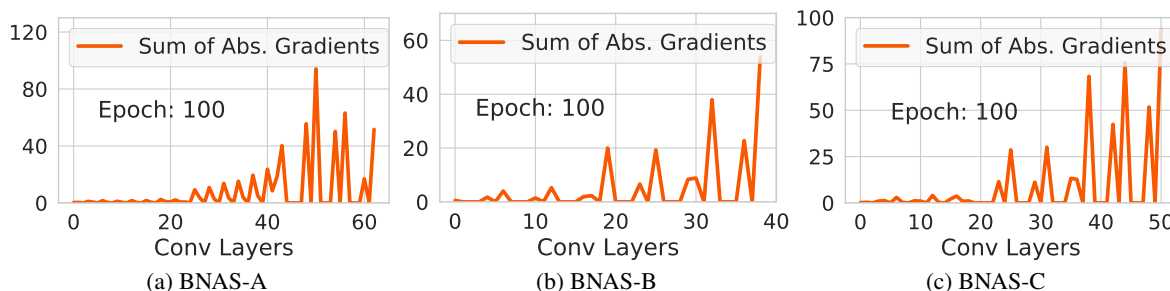


Figure 14: Unstable gradients in the ‘No Skip’ ablation (Similar to ‘w/o SC’ in Figure 4-(b)) of BNAS- $\{A,B,C\}$ models. We show the sum of gradient magnitudes for convolution layers in all three models for the *No Skip* setting. All three models show spiky gradients without the proposed skip-connections

Table 11: Plot details in ‘comb_grads.gif’ file. We provide an animated plot for ‘BNAS-A w/ SC’ for comparison to those of the other ablated models without the skip connection (BNAS-A w/o SC, BNAS-B w/o SC, BNAS-C w/o SC). Other models (BNAS-B and C) with skip connections show similar trend with BNAS-A, and thus omitted for clear presentation

Plot Title	Model	Skip Connections
BNAS-A w/ SC	BNAS-A	✓
BNAS-A w/o SC	BNAS-A	✗
BNAS-B w/o SC	BNAS-B	✗
BNAS-C w/o SC	BNAS-C	✗

Table 12: Comparing our searched binary networks (BNAS-A) with and without the *Zeroise* layer on CIFAR10. *Test Acc. (%)* indicates the test accuracy on CIFAR10. The two models compared have the exact same configuration except the usage of *Zeroise* layers in the search space. Note that the memory savings and inference speed-up were calculated with respect to the floating point version of BNAS-A without *Zeroise* since *Zeroise* layers are not used in floating point domain (see Section 7 for related discussion)

BNAS-A	w/o Zeroise	w/ Zeroise
# Cells/# Chn.	20 / 36	20 / 36
Memory Savings	31.79×	91.06×
FLOPs ($\times 10^8$)	0.36	0.14
Inference Speed-up	58.01×	149.14×
Test. Acc. (%)	89.47	92.70

Table 13: No dilated convolutions in the search space. *Test Acc. (%)* indicates the test accuracy on CIFAR10. *BNAS-A w/o Dil. Conv.* indicates the cell searched without dilated convolutions. The architectures perform similarly regardless of dilated convolutions being included or not

FLOPs ($\times 10^8$)	Model	Test Acc. (%)
~ 0.16	BNAS-A w/o Dil. Conv.	92.22
	BNAS-A (w/ Dil. Conv.)	92.70

Table 14: Memory savings and inference speed-up compared to floating point counter part of our searched binary network (models for ImageNet experiments). Note that the memory savings and inference speed-up differ for different networks, as described in [7]. The FLOPs, memory savings and inference speed-up for Bi-Real Net is from Table 3 in [11]. All our models achieve higher or comparable memory savings and inference speed-up compared to Bi-Real Net [11]

Model	BNAS-D	BNAS-E	BNAS-F	BNAS-G	BNAS-H	Bi-Real Net18	Bi-Real Net34
FLOPs ($\times 10^8$)	~ 1.48	~ 1.63	~ 1.78	~ 1.93	~ 6.56	~ 1.63	~ 1.93
Memory Savings	13.91×	14.51×	30.37×	14.85×	21.75×	11.14×	15.97×
Inference Speed-up	20.85×	21.15×	24.29×	19.34×	24.81×	11.06×	18.99×

6.5.2 ‘No Zeroise’ Setting

In addition to reducing the quantization error, the *Zeroise* layers has additional benefits of more memory savings, reduced FLOPs and more inference speed-up as it does not require any computation and has no learnable parameters.

We summarize the memory savings, FLOPs and inference speed-up of our BNAS-A model in Table 12 by comparing our BNAS-A model with and without *Zeroise* layers. With the *Zeroise* layers, not only does the accuracy increase, but we also observe significantly more memory savings and inference speed-up.

6.6 Impact of Dilated Convolutions in the Search Space

To see the impact of dilated convolutions [68] on the performance of our searched architectures, we search binary networks without the dilated convolutions in our search space. We qualitatively compare the searched cells with and without the dilated convolution layer types in Figure 15 and quantitatively compare them in Table 13. As shown in Table 13, the dilated convolutional layers contribute to the accuracy of the searched model with a marginal gain. Hence, the act of searching the architectures seem to play a bigger role than including specific layer types in the search space.

6.7 Exclusion of Separable Convolution

In Sec. 3, we claim two issues for the failure of binarized DARTS, SNAS and GDAS; 1) accumulation of quantization error due to separable convolutions, 2) the lack of inter-cell skip connections that makes propagating the gradients across multiple cells difficult. Particularly, for the first issue (*i.e.*, using separable convolutions accumulates quantization error repetitively), we proposed to exclude the separable convolutions from the search space. Here, we further investigate the

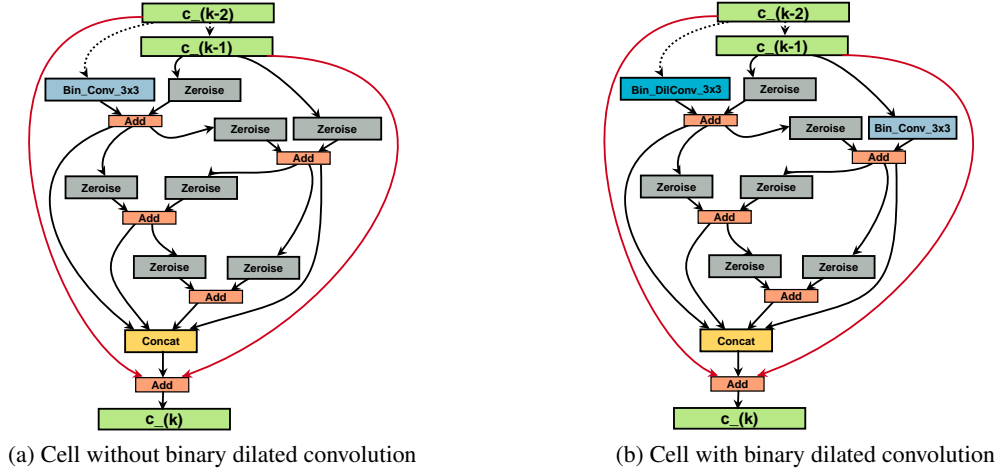


Figure 15: Comparing the cell searched with and without binary dilated convolutions in the search space. $c_{-}(k)$ indicates the output of the k^{th} cell. The dotted lines represents the connections from the second previous cell ($c_{-}(k-2)$). Red lines indicate the inter-cell skip connections

Table 15: Effect of separable convolutions in the search space. *Test Acc. (%)* refers to the test accuracy on CIFAR10. *Prop. of Sep. Conv.* refers to the percentage of separable convolutions in the searched convolutional cells. *BNAS-A w/ Sep. Conv.* refers to our searched network with separable convolutions included in the search space. *BNAS-A* refers to our searched network without separable convolutions in the search space. Note that the same binarization scheme (XNOR-Net) was applied in all methods. The models with higher proportion of separable convolutions show lower test accuracy. Please refer to Fig. 2 for the learning curves of DARTS + Binarized, SNAS + Binarized, GDAS + Binarized, and BNAS-A.

Method	Test Acc. (%)	Prop. of Sep. Conv. (%)
DARTS + Binarized	10.01	62.50
SNAS + Binarized	41.72	36.75
GDAS + Binarized	43.19	36.75
BNAS-A w/ Sep. Conv.	89.66	12.50
BNAS-A	92.70	0.00

accuracy of the searched architecture with the separable convolutions kept in the search space for binary networks and summarize the results in Table 15.

Since DARTS, SNAS, and GDAS search on the floating point domain, their search methods do not take quantization error into account and thus result in cells that have a relatively high percentage of separable convolutions and show low test accuracy. In contrast, we search directly on the binary domain which enables our search method to identify that separable convolutions have high quantization error and hence obtain a cell that contains very few separable convolution (*e.g.*, proportion of separable convolutions is 12.5% for BNAS while for others, it is higher than 36%). Note that explicitly excluding the separable convolutions from the search space does result in better performing binary architectures. The reason for the failure of separable convolutions is discussed in Sec. 4.1.2.

7 Memory Saving and Inference Speed-up

Following that other binary networks compare memory savings and inference speed-up with respect to their floating point counterpart [11], we compute the memory savings and inference speed-up by comparing it to the floating point version of our searched binary networks and summarize the results in Table 14 for the models for experiments with ImageNet dataset.

Note that all our models achieve higher or comparable memory savings and inference speed-up for the respective FLOPs budgets compared to Bi-Real models [11]. Specifically, our BNAS-D has $13.91\times$ memory savings and $20.85\times$ inference speed-up, which is higher than the usual savings and speed-up of around $11\times$ for other binary networks, while also outperforming other binary networks in terms of classification accuracy by large margins (please refer to Table 8).

8 Conclusion

To design better performing binary network architectures, we propose a method to search the space of binary networks, called BNAS. BNAS searches for a cell that can be stacked to generate networks for various computational budgets. To configure the feasible set of binary architectures, we define a new search space of binary layer types and a new cell template. Specifically, we propose to exclude separable convolution layer and include *Zeroise* layer type in the search space for less quantization error. In addition, we propose a new search objective with the diversity regularizer and show that it helps in obtaining better binary architectures. The learned architectures outperform the architectures used in the state-of-the-art binary networks on both CIFAR-10 and ImageNet.

Further, we observe an underfitting problem in our searched architectures when trained with the standard training scheme and propose a simpler training scheme that outperforms the state of the art binary networks by better fitting to the training data. Our architectures with our proposed training scheme outperform all hand-crafted binary networks in the literature and performs *on par* with the recently proposed searched network, BATS, with much less training efforts that are easily reproducible.

References

- [1] Song Han, Jeff Pool, John Tran, and William Dally. Learning both weights and connections for efficient neural network. In *NIPS*, 2015. 1
- [2] Xiangyu Zhang, Xinyu Zhou, Mengxiao Lin, and Jian Sun. Shufflenet: An extremely efficient convolutional neural network for mobile devices. In *CVPR*, 2018. 1
- [3] Forrest N. Iandola, Song Han, Matthew W. Moskewicz, Khalid Ashraf, William J. Dally, and Kurt Keutzer. SqueezeNet: Alexnet-level accuracy with 50x fewer parameters and <0.5mb model size. *arXiv:1602.07360*, 2016. 1
- [4] Andrew G Howard, Menglong Zhu, Bo Chen, Dmitry Kalenichenko, Weijun Wang, Tobias Weyand, Marco Andreetto, and Hartwig Adam. Mobilenets: Efficient convolutional neural networks for mobile vision applications. *arXiv preprint arXiv:1704.04861*, 2017. 1, 6
- [5] Max Jaderberg, Andrea Vedaldi, and Andrew Zisserman. Speeding up convolutional neural networks with low rank expansions. *arXiv preprint arXiv:1405.3866*, 2014. 1
- [6] Matthieu Courbariaux, Yoshua Bengio, and Jean-Pierre David. Binaryconnect: Training deep neural networks with binary weights during propagations. In *NIPS*, 2015. 1, 3
- [7] Mohammad Rastegari, Vicente Ordonez, Joseph Redmon, and Ali Farhadi. Xnor-net: Imagenet classification using binary convolutional neural networks. In *ECCV*, 2016. 1, 2, 3, 5, 6, 13, 15, 16, 19
- [8] Fengfu Li, Bo Zhang, and Bin Liu. Ternary weight networks. *arXiv preprint arXiv:1605.04711*, 2016. 1, 3
- [9] Geoffrey Hinton, Oriol Vinyals, and Jeff Dean. Distilling the knowledge in a neural network. *arXiv preprint arXiv:1503.02531*, 2015. 1
- [10] Sarah Tan, Rich Caruana, Giles Hooker, Paul Koch, and Albert Gordo. Learning global additive explanations for neural nets using model distillation. *arXiv preprint arXiv:1801.08640*, 2018. 1
- [11] Zechun Liu, Baoyuan Wu, Wenhan Luo, Xin Yang, Wei Liu, and Kwang-Ting Cheng. Bi-real net: Enhancing the performance of 1-bit cnns with improved representational capability and advanced training algorithm. In *ECCV*, 2018. 1, 3, 12, 13, 15, 16, 19, 20
- [12] Chunlei Liu, Yue Qi, Xue Xia, Baochang Zhang, Jiabin Gu, Jianzhuang Liu, Rongrong Ji, and David S. Doermann. Circulant binary convolutional networks: Enhancing the performance of 1-bit dnns with circulant back propagation. In *CVPR*, 2019. 1, 3, 15, 16
- [13] Mingzhu Shen, Kai Han, Chunjing Xu, and Yunhe Wang. Searching for accurate binary neural architectures. In *ICCV Workshop*, 2019. 1, 3, 13
- [14] Hanxiao Liu, Karen Simonyan, and Yiming Yang. DARTS: Differentiable architecture search. In *ICLR*, 2019. 1, 4, 5, 6, 7, 8, 9, 12, 13
- [15] Sirui Xie, Hehui Zheng, Chunxiao Liu, and Liang Lin. SNAS: stochastic neural architecture search. In *ICLR*, 2019. 1, 4, 5
- [16] Xuanyi Dong and Yi Yang. Searching for a robust neural architecture in four gpu hours. In *CVPR*, 2019. 1, 4, 5
- [17] Ruizhou Ding, Ting-Wu Chin, Zeye Liu, and Diana Marculescu. Regularizing activation distribution for training binarized deep networks. In *CVPR*, pages 11408–11417, 2019. 2, 3, 9, 10

- [18] Haotong Qin, Ruihao Gong, Xianglong Liu, Mingzhu Shen, Ziran Wei, Fengwei Yu, and Jingkuan Song. Forward and backward information retention for accurate binary neural networks. In *CVPR*, pages 2250–2259, 2020. 2, 4, 9, 10
- [19] Chenzhuo Zhu, Song Han, Huizi Mao, and William J Dally. Trained ternary quantization. *arXiv preprint arXiv:1612.01064*, 2016. 3
- [20] Matthieu Courbariaux, Itay Hubara, Daniel Soudry, Ran El-Yaniv, and Yoshua Bengio. Binarized neural networks: Training deep neural networks with weights and activations constrained to+ 1 or-1. *arXiv preprint arXiv:1602.02830*, 2016. 3, 8, 16
- [21] Shuchang Zhou, Yuxin Wu, Zekun Ni, Xinyu Zhou, He Wen, and Yuheng Zou. Dorefa-net: Training low bitwidth convolutional neural networks with low bitwidth gradients. *arXiv preprint arXiv:1606.06160*, 2016. 3
- [22] Xiaofan Lin, Cong Zhao, and Wei Pan. Towards accurate binary convolutional neural network. In *NIPS*, 2017. 3, 12, 16
- [23] Diwen Wan, Fumin Shen, Li Liu, Fan Zhu, Jie Qin, Ling Shao, and Heng Tao Shen. Tbn: Convolutional neural network with ternary inputs and binary weights. In *ECCV*, 2018. 3
- [24] Ziwei Wang, Jiwen Lu, Chenxin Tao, Jie Zhou, and Qi Tian. Learning channel-wise interactions for binary convolutional neural networks. In *CVPR*, 2019. 3
- [25] Jiaxin Gu, Ce Li, Baochang Zhang, Jungong Han, Xianbin Cao, Jianzhuang Liu, and David Doermann. Projection convolutional neural networks for 1-bit cnns via discrete back propagation. In *AAAI*, 2019. 3, 12, 16
- [26] Adrian Bulat and Georgios Tzimiropoulos. Xnor-net++: Improved binary neural networks. In *BMVC*, 2019. 3, 16
- [27] Felix Juefei-Xu, Vishnu Naresh Boddeti, and Marios Savvides. Local binary convolutional neural networks. In *CVPR*, 2017. 3
- [28] Shilin Zhu, Xin Dong, and Hao Su. Binary ensemble neural network: More bits per network or more networks per bit? In *CVPR*, 2019. 3
- [29] Hai Phan, Dang Huynh, Yihui He, Marios Savvides, and Zhiqiang Shen. Mobinet: A mobile binary network for image classification. *arXiv preprint arXiv:1907.12629*, 2019. 3
- [30] Bohan Zhuang, Chunhua Shen, Mingkui Tan, Lingqiao Liu, and Ian Reid. Structured binary neural networks for accurate image classification and semantic segmentation. In *CVPR*, 2019. 3
- [31] Dahyun Kim, Kunal Pratap Singh, and Jonghyun Choi. Learning architectures for binary networks. In *ECCV*, 2020. 3, 4, 9
- [32] Adrian Bulat, Brais Martínez, and Georgios Tzimiropoulos. Bats: Binary architecture search. In *ECCV*, 2020. 3, 10, 16, 17
- [33] Bohan Zhuang, Chunhua Shen, Mingkui Tan, Lingqiao Liu, and Ian Reid. Towards effective low-bitwidth convolutional neural networks. In *CVPR*, 2018. 3
- [34] Jiaxin Gu, Junhe Zhao, Xiaolong Jiang, Baochang Zhang, Jianzhuang Liu, Guodong Guo, and Rongrong Ji. Bayesian optimized 1-bit cnns. In *CVPR*, 2019. 3, 16
- [35] Zechun Liu, Zhiqiang Shen, Marios Savvides, and Kwang-Ting Cheng. Reactnet: Towards precise binary neural network with generalized activation functions. In *European Conference on Computer Vision (ECCV)*, 2020. 3
- [36] Mingbao Lin, Rongrong Ji, Zihan Xu, Baochang Zhang, Yan Wang, Yongjian Wu, Feiyue Huang, and Chia-Wen Lin. Rotated binary neural network. *arXiv preprint arXiv:2009.13055*, 2020. 4
- [37] Hyungjun Kim, Kyungsu Kim, Jinseok Kim, and Jae-Joon Kim. Binaryduo: Reducing gradient mismatch in binary activation network by coupling binary activations. In *ICLR*, 2020. 4, 15, 16
- [38] Brais Martinez, Jing Yang, Adrian Bulat, and Georgios Tzimiropoulos. Training binary neural networks with real-to-binary convolutions. In *International Conference on Learning Representations*, 2020. 4, 9, 17
- [39] Barret Zoph, Vijay Vasudevan, Jonathon Shlens, and Quoc V. Le. Learning transferable architectures for scalable image recognition. In *CVPR*, 2018. 4, 5, 8
- [40] Barret Zoph and Quoc V. Le. Neural architecture search with reinforcement learning. In *ICLR*, 2017. 4
- [41] Hieu Pham, Melody Guan, Barret Zoph, Quoc Le, and Jeff Dean. Efficient neural architecture search via parameters sharing. In *ICML*, 2018. 4
- [42] Xin Chen, Lingxi Xie, Jun Wu, and Qi Tian. Progressive differentiable architecture search: Bridging the depth gap between search and evaluation. In *ICCV*, pages 1294–1303, 2019. 4

- [43] Han Cai, Ligeng Zhu, and Song Han. ProxylessNAS: Direct neural architecture search on target task and hardware. In *ICLR*, 2019. 4
- [44] Gabriel Bender, Pieter-Jan Kindermans, Barret Zoph, Vijay Vasudevan, and Quoc Le. Understanding and simplifying one-shot architecture search. In *ICML*, 2018. 4
- [45] Renqian Luo, Fei Tian, Tao Qin, Enhong Chen, and Tie-Yan Liu. Neural architecture optimization. In *NIPS*. 2018. 4
- [46] Chenxi Liu, Liang-Chieh Chen, Florian Schroff, Hartwig Adam, Wei Hua, Alan L. Yuille, and Li Fei-Fei. Auto-deeplab: Hierarchical neural architecture search for semantic image segmentation. In *CVPR*, 2019. 4
- [47] Bichen Wu, Xiaoliang Dai, Peizhao Zhang, Yanghan Wang, Fei Sun, Yiming Wu, Yuandong Tian, Peter Vajda, Yangqing Jia, and Kurt Keutzer. Fbnet: Hardware-aware efficient convnet design via differentiable neural architecture search. In *CVPR*, 2019. 4
- [48] Yanqi Zhou, Siavash Ebrahimi, Sercan Ö Arık, Haonan Yu, Hairong Liu, and Greg Diamos. Resource-efficient neural architect. *arXiv preprint arXiv:1806.07912*, 2018. 4
- [49] Chenxi Liu, Barret Zoph, Maxim Neumann, Jonathon Shlens, Wei Hua, Li-Jia Li, Li Fei-Fei, Alan Yuille, Jonathan Huang, and Kevin Murphy. Progressive neural architecture search. In *ECCV*, 2018. 4
- [50] Jin-Dong Dong, An-Chieh Cheng, Da-Cheng Juan, Wei Wei, and Min Sun. Dpp-net: Device-aware progressive search for pareto-optimal neural architectures. In *ECCV*, 2018. 4
- [51] Hanxiao Liu, Karen Simonyan, Oriol Vinyals, Chrisantha Fernando, and Koray Kavukcuoglu. Hierarchical representations for efficient architecture search. In *ICLR*, 2018. 4
- [52] Chris Zhang, Mengye Ren, and Raquel Urtasun. Graph hypernetworks for neural architecture search. In *ICLR*, 2019. 4
- [53] Saining Xie, Alexander Kirillov, Ross Girshick, and Kaiming He. Exploring randomly wired neural networks for image recognition. *arXiv preprint arXiv:1904.01569*, 2019. 4
- [54] Liam Li and Ameet Talwalkar. Random search and reproducibility for neural architecture search. *arXiv preprint arXiv:1902.07638*, 2019. 4
- [55] Mingxing Tan and Quoc V. Le. Efficientnet: Rethinking model scaling for convolutional neural networks. In *ICML*, 2019. 4
- [56] Eric Jang, Shixiang Gu, and Ben Poole. Categorical reparameterization with gumbel-softmax. In *ICLR*, 2017. 4
- [57] Yukang Chen, Gaofeng Meng, Qian Zhang, Xinbang Zhang, Liangchen Song, Shiming Xiang, and Chunhong Pan. Joint neural architecture search and quantization. *ArXiv*, abs/1811.09426, 2018. 4
- [58] Kuan Wang, Zhijian Liu, Yujun Lin, Ji Lin, and Song Han. Haq: Hardware-aware automated quantization with mixed precision. In *CVPR*, 2019. 4
- [59] Bichen Wu, Yanghan Wang, Peizhao Zhang, Yuandong Tian, Peter Vajda, and Kurt Keutzer. Mixed precision quantization of convnets via differentiable neural architecture search. *ArXiv*, abs/1812.00090, 2018. 4
- [60] Qian Lou, Lantao Liu, Minje Kim, and Lei Jiang. Autoqb: Automl for network quantization and binarization on mobile devices. *ArXiv*, abs/1902.05690, 2019. 4
- [61] Hanlin Chen, Li'an Zhuo, Baochang Zhang, Xiawu Zheng, Jianzhuang Liu, David S. Doermann, and Rongrong Ji. Binarized neural architecture search. *ArXiv*, abs/1911.10862, 2019. 4
- [62] Laurent Sifre and Stéphane Mallat. Rigid-motion scattering for image classification. 6
- [63] A. Krizhevsky. Learning Multiple Layers of Features from Tiny Images. Technical report, 2009. 12
- [64] Olga Russakovsky, Jia Deng, Hao Su, Jonathan Krause, Sanjeev Satheesh, Sean Ma, Zhiheng Huang, Andrej Karpathy, Aditya Khosla, Michael Bernstein, et al. Imagenet large scale visual recognition challenge. *IJCV*, 115(3):211–252, 2015. 12
- [65] Ilya Loshchilov and Frank Hutter. Sgdr: Stochastic gradient descent with warm restarts. *arXiv preprint arXiv:1608.03983*, 2016. 12
- [66] Leslie N Smith. A disciplined approach to neural network hyper-parameters: Part 1—learning rate, batch size, momentum, and weight decay. *arXiv preprint arXiv:1803.09820*, 2018. 12
- [67] Sergey Zagoruyko and Nikos Komodakis. Paying more attention to attention: Improving the performance of convolutional neural networks via attention transfer. *ICLR*, 2017. 17
- [68] Fisher Yu and Vladlen Koltun. Multi-scale context aggregation by dilated convolutions. 2016. 19